BILINGUAL PUBLISHING CO.
Pioneer of Global Academics Since 1984

Journal of Environmental & Earth Sciences
https://ojs.bilpublishing.com/index.php/jees

ARTICLE

Power Spectrum in the Conductive Terrestrial Ionosphere

Georgi Jandieri* **Jaromir Pistora** **Nino Mchedlishvili**

International Space Agency Society Georgia, Tbilisi, 0184, Georgia

ARTICLE INFO

Article history
Received: 19 March 2020
Accepted: 23 March 2020
Published Online: 31 March 2020

Keywords:
Ionosphere
Turbulence
Irregularities
Plasma scattering

ABSTRACT

Stochastic differential equation of the phase fluctuations is derived for the collision conductive magnetized plasma in the polar ionosphere applying the complex geometrical optics approximation. Calculating second order statistical moments it was shown that the contribution of the longitudinal conductivity substantially exceeds both Pedersen and Hall's conductivities. Experimentally observing the broadening of the spatial power spectrum of scattered electromagnetic waves which equivalent to the brightness is analyzed for the elongated ionospheric irregularities. It was shown that the broadening of the spectrum and shift of its maximum in the plane of the location of an external magnetic field (main plane) less than in perpendicular plane for plasmonic structures having linear scale tenth of kilometer; and substantially depends on the penetration angle of an incident wave in the conductive collision turbulent magnetized ionospheric plasma. The angle-of-arrival (AOA) in the main plane has the asymmetric Gaussian form while in the perpendicular plane increases at small anisotropy factors and then tends to the saturation for the power-low spectrum characterizing electron density fluctuations. Longitudinal conductivity fluctuations increase the AOAs of scattered radiation than in magnetized plasma with permittivity fluctuations. Broadening of the temporal spectrum containing the drift velocity of elongated ionospheric irregularities in the polar ionosphere allows to solve the reverse problem restoring experimentally measured velocity of the plasma streams and characteristic linear scales of anisotropic irregularities in the terrestrial ionosphere.

1. Introduction

Radiation of electromagnetic waves in the ionospheric plasma is of great interest from both a theoretical and practical point of view. The geomagnetic field plays a key role in both the dynamic processes in the terrestrial ionosphere and irregularities having different spatial scales usually elongated along the lines of force of the geomagnetic field. Statistical methods have been proposed to treat radiation in randomly inhomogeneous media [1,2].

Phase structure functions and the angle-of-arrival (AOA) of scattered electromagnetic waves in the turbulent magnetized plasma have been considered in [3,4] applying the stochastic eikonal equation. Investigation of the statistical moments in the turbulent conductive ionospheric plasma is of practical importance. Collision between plasma particles leads to the absorption of scattered radio waves. Components of the conductivity tensor in the homogeneous medium have been obtained [5] account being taken both declination and inclination angles of the

**Corresponding Author:*
George Jandieri,
International Space Agency Society Georgia, Tbilisi, Georgia, 0184;
Email: giorgijandieri7@mail.ru

 DOI: https://doi.org/10.30564/jees.v2i1.1763

geomagnetic field. Second order statistical moments of a scattered radiation in the collision magnetized plasma were considered analytically and numerically in [6].

In the present work, section 2, the dispersion equation is derived calculating attenuation of oblique incident plane electromagnetic wave penetrating in a conductive homogeneous collision magnetized plasma. In section 3 stochastic differential equation of the phase fluctuations is derived account being taken both dielectric permittivity and conductivity fluctuations satisfying the boundary conditions. Second order statistical moment – phase correlation function of scattered radiation is obtained for arbitrary correlation function of electron density fluctuations. Broadening of both the spatial power spectrum (SPS) and temporal spectrum of scattered electromagnetic waves are investigated analytically in the conductive collision ionospheric plasma with randomly varying magnetoionic parameters using the complex geometrical optics approximation. Numerical calculations are carried out in Section 4 for modified spectral function containing both anisotropic Gaussian and power-law correlation functions of electron density fluctuations including both the anisotropy factor and the inclination angle of elongated ionospheric irregularities with respect to the geomagnetic lines of force using the experimental data. Results and discussions are given in Section 5.

2. Formulation of the Problem

Vector of the electric field $\mathbf{E}$ satisfies the wave equation:

$$\left\{ \nabla_i \nabla_j - \Delta\delta_{ij} - k_0^2\ \tilde{\varepsilon}_{ij}(\mathbf{r}) \right\} \mathbf{E_j}(\mathbf{r}) = 0\ , \qquad (1)$$

where: $k_0 = \omega / c$ is the wavenumber of an incident wave with frequency ω; Δ is the Laplacian, δ_{ij} is the Kronecker symbol, $\tilde{\varepsilon}_{ij} = \varepsilon_{ij} - i\,\tilde{\sigma}_{ij}$, $\tilde{\sigma}_{ij} \equiv \sigma_{ij}\ (4\pi / k_0\, c)$ are the second rank permittivity and conductivity tensors of the turbulent conductive collision turbulent magnetized plasma, respectively, which are random functions of the spatial coordinates.

The ambient external magnetic field $\mathbf{H_0}$ is directed vertically upwards along the Z-axis (polar ionosphere), wave vector of a refractive plane electromagnetic wave in the absorptive random medium is located in the YOZ plane (main plane) of the Cartesian coordinate system. We suppose that $s^2 << (1-\sqrt{u})^2$. Components of the second rank permittivity tensor and conductivity tensors of the magnetized plasma are [7,8]:

$$\tilde{\varepsilon}_{xx} = \tilde{\varepsilon}_{yy} = \tilde{\eta} - i\,\eta'\ ,\ \tilde{\varepsilon}_{xy} = -\tilde{\varepsilon}_{yx} = \mu' - \mu\ ,\ \tilde{\varepsilon}_{zz} = \tilde{\zeta} - i\,\zeta'$$

where: $\tilde{\eta} = 1 - \Delta$, $\eta' = s\,\Delta_1\,(1+u) + \tilde{\sigma}_\perp$, $\mu' = 2\,s\,\Delta_1\sqrt{u}$,

$$\tilde{\mu} = \Delta\sqrt{u} + \tilde{\sigma}_H\ ,\quad \tilde{\zeta} = 1 - \mathrm{v}\ ,\quad \zeta' = s\,\mathrm{v} + \tilde{\sigma}_\parallel\ ,$$

$$\sigma_\parallel = e^2 N \left(\frac{1}{m_e\,\nu_e} + \frac{1}{m_m\,\nu_i} \right),$$

$$\sigma_\perp = e^2 N \left(\frac{\nu_e}{m_e\,(\nu_e^2 + \omega_e^2)} + \frac{\nu_i}{m_i\,(\nu_i^2 + \omega_i^2)} \right),$$

$$\sigma_H = e^2 N \left(\frac{\omega_e}{m_e\,(\nu_e^2 + \omega_e^2)} - \frac{\omega_i}{m_i\,(\nu_{in}^2 + \omega_i^2)} \right),$$

$\Delta \equiv \mathrm{v}/(1-u)$, $\Delta_1 \equiv \mathrm{v}/(1-u)^2$, $\mathrm{v}(\mathbf{r}) = \omega_p^2(\mathbf{r})/\omega^2$ and $u = (e\,H_0 / m_e\,c\,\omega)^2$ are magneto-ionic parameters of the ionospheric plasma, $\omega_p(\mathbf{r}) = \left[4\pi N_e(\mathbf{r})\, e^2 / m_e \right]^{1/2}$ is the plasma frequency, $N_e(\mathbf{r})$ is the electron density which is a random function of the spatial coordinates, e and m_e are the charge and mass of an electron, c is the speed of light in vacuum, $s = \nu_{eff} / \omega$ is the collision frequency between plasma particles; $\sigma_\parallel$, $\sigma_\perp$ and σ_H are the longitudinal, transverse (Pedersen) and Hall's conductivities, respectively, $\nu_{e,i}$ is the electron or ion collision frequency with the neutral molecules, ω_e and ω_i are the angular gyrofrequencies of an electron and ion, respectively; m_i is the mass of ion. At high frequencies the influence of ions can be neglected.

If oblique incident plane wave penetrates into homogeneous conductive collision magnetized plasma at arbitrary refractive angle θ to the external magnetic field $\mathbf{H_0}$ from equation (1) we obtain set of equations:

$$(t_2^2 + t^2 - \tilde{\varepsilon}_{xx})\,E_x - (t_1\,t_2 + \tilde{\varepsilon}_{xy})E_y - t_1\,t\,E_z = 0\ ,$$

$$(t_1\,t_2 + \tilde{\varepsilon}_{yx})E_x - (t_1^2 + t^2 - \tilde{\varepsilon}_{yy})\,E_y + t_2\,t\,E_z = 0\ ,$$

$$t_1\,t\,E_x + t_2\,t\,E_y - (t_1^2 + t_2^2 - \tilde{\varepsilon}_{zz})\,E_z = 0\ , \qquad (3)$$

where: $k_x = k_0\,\tilde{N}\sin\theta\,\sin\varphi = k_0\,t_1$, $t_1^2 + t_2^2 + t^2 = \tilde{N}^2$,

$k_y = k_0\,\tilde{N}\sin\theta\cos\varphi = k_0\,t_2$, $k_z = k_0\,\tilde{N}\cos\varphi = k_0\,t$;

φ is the polar angle between the projection of an incident

DOI: https://doi.org/10.30564/jees.v2i1.1763

wavevector $\mathbf{k_0}$ on the XOY plane and the Y axis. Complex refractive index [9] of the collision magnetized plasma: $N^2 = (N - i\text{æ})^2 = N_1^2 - i N_2^2$ contains the refractive coefficient of homogeneous plasma N_* and the absorption coefficient æ :

$$N_1^2 = 1 - 2\frac{\mathrm{v}(1-\mathrm{v})}{\Upsilon}, N_2^2 = s\frac{\mathrm{v}}{\Upsilon^2}[\Delta + 2(1-\mathrm{v})(\mathrm{v}-2)], \quad (4)$$

where: $\Upsilon = 2(1-\mathrm{v}) - u\sin^2\theta \pm \left[u^2\sin^4\theta + 4u(1-\mathrm{v})^2 \cdot \right.$

$\left. \cdot \cos^2\theta\right]^{1/2}$, signs $"\pm"$ corresponds to the ordinary and extraordinary waves. Determinant set of equations (3) is:

$$t^4 + (D_1 + i D_2)\, t^2 + (D_3 + i D_4) = 0 \ , \quad (5)$$

where: $D_1 + i D_2 = \left[(C_1\tilde{\xi} - C_2\zeta') + i\,(C_1\zeta' + C_2\tilde{\xi})\right] \cdot$

$(\tilde{\xi}^2 + \zeta'^2)^{-1}$,

$D_3 + i D_4 = \left[(e_1\tilde{\xi} - e_2\zeta') + i\,(e_1\zeta' + e_2\tilde{\xi})\right] \cdot (\tilde{\xi}^2 + \zeta'^2)^{-1}$,

$C_1 = \left[N_1^2(\tilde{\eta} + \tilde{\xi}) - N_2^2(\eta' + \zeta')\right]\sin^2\theta - 2(\tilde{\eta}\tilde{\xi} - \eta'\zeta')$,

$C_2 = 2(\tilde{\eta}\zeta' + \tilde{\xi}\eta') - \left[N_1^2(\eta' + \zeta') + N_2^2(\tilde{\eta} + \tilde{\xi})\right]\sin^2\theta$,

$e_1 = (N_1^2\sin^2\theta - \tilde{\xi})(N_1^2\tilde{\eta}\sin^2\theta - \tilde{\eta}^2 + \eta'^2 + \tilde{\mu}^2) -$

$N_2^4\tilde{\eta}\sin^4\theta - \zeta'(2\tilde{\eta}\eta' + 2\tilde{\mu}\mu' - N_1^2\eta'\sin^2\theta) -$

$N_2^2\sin^2\theta - \left[(N_1\sin^2\theta - \tilde{\xi})\eta' + N_1^2\eta'\sin^2\theta - 2\tilde{\eta}\eta' -\right.$

$\left. - 2\tilde{\mu}\mu' - \tilde{\eta}\zeta'\right]$,

$e_2 = (N_1^2\sin^2\theta - \tilde{\xi})(-N_1^2\eta'\sin^2\theta + 2\tilde{\eta}\eta' + 2\tilde{\mu}\mu') +$

$+ N_2^4\eta'\sin^4\theta + \zeta'(N_1^2\tilde{\eta}\sin^2\theta - \tilde{\eta}^2 + \eta'^2 + \tilde{\mu}^2) -$

$- N_2^2\sin^2\theta\left[(N_1\sin^2\theta - \tilde{\xi})\tilde{\eta} + N_1^2\tilde{\eta}\sin^2\theta - \tilde{\eta}^2 + \right.$

$\left. + \eta'^2 + \tilde{\mu}^2) + N_2^2\zeta'\eta'\sin^2\theta\right]$.

The solution of equation (5) k_z / k_0 determines the attenuation of an incident wave propagating in the collision conductive homogeneous plasma for arbitrary angle θ.

3. Statistical Moments in the Conductive Collision Magnetized Plasma

In this section calculating the statistical characteristics of scattered electromagnetic waves we suppose that the characteristic spatial scale of elongated ionospheric irregularities exceeds the wavelength λ of an incident wave. This assumption enables to use the complex geometrical optics approximation ignoring the interaction between the normal waves account being taken that the phase fluctuations substantially exceed the amplitude fluctuations. Application of this method impose well-known restrictions on the distance traveled by the wave in the inhomogeneous medium. Wave field introduce as [9]

$E_i(\mathbf{r}) = A_i(\mathbf{r})\exp\left[i\,\varphi(\mathbf{r})\right]$, $\varphi(\mathbf{r}) = k_0\,\tilde{N}(\boldsymbol{\tau}\,\mathbf{r}) + \varphi_1(\mathbf{r}) =$

$= k_0\,\tilde{N}(y\sin\theta + z\cos\theta) + \varphi_1(\mathbf{r})$, (6)

here: $\varphi_1(\mathbf{r})$ is the phase fluctuation of a scattered wave, $N_e(\mathbf{r}) = N_{e0}(1 + n_1(\mathbf{r}))$, N_{e0} is constant value, $n_1(\mathbf{r})$ is a random function of the spatial coordinates. Dielectric permittivity is a sum of the constant mean and fluctuating terms $\tilde{\varepsilon}_{ik} = <\tilde{\varepsilon}_{ik}> + \tilde{\varepsilon}'_{ik}$ ($<\tilde{\varepsilon}_{ik}> >> \tilde{\varepsilon}'_{ik}$, the angular brackets indicate the ensemble average). The second term contains $n_1(\mathbf{r})$ can be obtained from equation (1).

Substituting equation (6) into (1) fluctuating phase satisfies stochastic differential equations:

$$(\tilde{a}_z + i a'_z)\frac{\partial\varphi_1}{\partial z} + (\tilde{a}_y + i a'_y)\frac{\partial\varphi_1}{\partial y} = k_0\,(\tilde{A} + i A')\,n_1(\mathbf{r}), \quad (7)$$

where: $\tilde{a}_y = N_1\sin\theta\left[(\tilde{\eta} - N_1^2)(\tilde{\eta} + \tilde{\xi}) + N_1^2(\tilde{\xi} - \tilde{\eta})\sin^2\theta\right.$

$\left. - \tilde{\mu}^2\right]$, $\tilde{a}_z = N_1\cos\theta\left[2\tilde{\xi}(\tilde{\eta} - N_1^2) + N_1^2(\tilde{\xi} - \tilde{\eta})\sin^2\theta\right]$,

$a'_y = N_1\sin\theta\left\{(\tilde{\eta} + \tilde{\xi})(N_2^2 - \eta') - (\tilde{\eta} - N_1^2)(\eta' + \zeta') +\right.$

$$+\left[N_1^2(\eta'-\zeta')-N_2^2(\tilde{\xi}-\tilde{\eta})\right]\sin^2\theta-2\mu'\tilde{\mu}\Big\},$$

$$a_z'=N_1\cos\theta\left\{2\left[\tilde{\zeta}(N_2^2-\eta')-(\tilde{\eta}-N_1^2)\right]+\right.$$

$$\left.+\sin^2\theta\left[N_1^2(\eta'-\zeta')-N_2^2(\tilde{\zeta}-\tilde{\eta})\right]\right\},$$

$$\tilde{A}=(N_1^4-6N_1^2N_2^2)(\zeta_1\cos^2\theta+\eta_1\sin^2\theta)+4N_1^3N_2$$

$$\cdot(\zeta'\cos^2\theta+\eta'\sin^2\theta)-(N_1^2-N_2^2)\Big[(1+\cos^2\theta)(\tilde{\eta}\zeta_1'+$$

$$+\zeta_1\eta'+\tilde{\zeta}\eta_1'-\zeta'\eta_1)+2\sin^2\theta(\tilde{\eta}\eta_1'-\eta'\eta_1+\tilde{\mu}\mu')\Big]+$$

$$+2N_1N_2(1+\cos^2\theta)(\eta'\zeta_1'-\tilde{\eta}\zeta_1+\zeta'\eta_1'+\tilde{\zeta}\eta_1)+$$

$$+2N_1N_2\sin^2\theta(2\eta'\eta_1'+2\tilde{\eta}\eta_1-\mu'^2+\tilde{\mu}^2)-(\tilde{\eta}^2-\eta'^2)$$

$$\cdot\zeta_1-2\tilde{\eta}\eta'\zeta_1'-(\mu'^2-\tilde{\mu}^2)\zeta_1-2\tilde{\mu}\mu'\zeta_1'2(\tilde{\eta}\tilde{\zeta}-\eta'\zeta')\cdot$$

$$\cdot\eta_1'+2(\tilde{\eta}\tilde{\zeta}-\eta'\zeta')\eta_1'-2(\tilde{\eta}\zeta'+\tilde{\zeta}\eta')\eta_1+(\mu'^2-\tilde{\mu}^2)\cdot$$

$$\cdot\zeta'+2\tilde{\mu}\tilde{\zeta}\mu'.$$

Double Fourier transformation and the boundary condition $\tilde{\varphi}_1|_{z=0}=0$ yield the solution of equation (7):

$$\tilde{\varphi}_1(x,y,z)=k_0(D+iE)\int_{-\infty}^{\infty}dk_x\int_{-\infty}^{\infty}dk_y\exp(ik_xx+ik_yy)$$

$$\int_0^L d\xi\, n_1(k_x,k_y,L)\exp\left[(-a+ib)(\xi-L)k_y\right], \qquad (8)$$

here L is the distance propagating by the wave in the conductive collision magnetized plasma satisfying the condition $ak_0L<<k_0l$ (l is the characteristic spatial scale of electron density fluctuations), coefficients: a, b, D and E are:

$$-a+ib=\frac{tg\,\theta}{\Psi_3}(-\Psi_1+i\,\Psi_2)\,tg\theta,$$

$$D+iE=\frac{1}{\Psi_3\,2N_1\cos\theta}(\Psi_4+i\,\Psi_5), \qquad (9)$$

where: $\Psi_1=a_y'\tilde{a}_z-\tilde{a}_y a_z'$, $\Psi_1=\tilde{a}_y\tilde{a}_z+a_y'a_z'$,

$$\Psi_3=\tilde{a}_z^2+a_z'^2,\ \Psi_4=\tilde{A}\tilde{a}_z+A'a_z',\ \Psi_5=A'\tilde{a}_z-\tilde{A}a_z'.$$

If wave propagates along the ambient external magnetic field ($\theta=0$) $-a+ib=0$, i.e. no dumping caused due to conductivity fluctuations; at angle $\theta=45^0$ we obtain $-a+ib=\pm0.02+0.67i$. Scattered electromagnetic waves dumped stronger in proportion to the angle θ.

Correlation function of the phase fluctuations is:

$$V_\varphi(\rho_x,\rho_y,\rho_z)=<\tilde{\varphi}_1(x+\rho_x,y+\rho_y,\rho_z)\tilde{\varphi}_1^*(x,y,\rho_z)>$$

$$=2\pi k_0^2(D^2+E^2)\int_{-\infty}^{\infty}dk_x\int_{-\infty}^{\infty}dk_y\,W_N(k_x,k_y,-bk_y)\frac{1}{2ak_y}$$

$$\left[1-\exp(-2ak_y\rho_z)\right]\exp(ik_x\rho_x+ik_y\rho_y+ik_z\rho_z), \qquad (10)$$

where k_x and k_y are components of the wavevector perpendicular to the external magnetic field, ρ_x and ρ_y are the distances between observation points spaced apart at a small distance in the main and perpendicular planes, respectively. The regular phase difference between two observation points are neglected. Equation (10) includes both field-aligned $l_\parallel$ and transversal $l_\perp$ characteristics linear scales of anisotropic electron density irregularities. If $ak_y\rho_z<1$, exponential term in (10) can be expended into a series. In this case statistical characteristics of the phase fluctuations are proportion to the distance L travelling by the wave in the turbulent plasma. This statement is valid beyond of its application [1,2].

In the theory of waves propagation in the turbulent ionosphere usually are interested in both amplitude and phase fluctuations, however in different type systems the registering parameter is the frequency. In general, the intensity of frequency fluctuations of scattered electromagnetic waves depends on: 1) the geometry of the task (thickness of a turbulent conductive collision magnetized plasma slab, angle between the wave vector of an incident wave and the ambient magnetic field; 2) characteristics spatial scale of elongated plasmonic structures (account being taken anisotropy factor and the inclination angle of ionospheric irregularities with respect to the external magnetic field); 3) absorption caused by the collision of electrons

DOI: https://doi.org/10.30564/jees.v2i1.1763

with other plasma particles. In this case frequency fluctuations caused due to scattering on the turbulent plasmonic structures put natural restrictions on the accuracy of measurements.

The spatial power spectrum (SPS) is the 3D Fourier transformation of the correlation function of a scattered radiation [2]. This second-order statistical moment is equivalent to the brightness which usually enters the radiation transport equation. It is characterized by broadening in the main YOZ and perpendicular planes [3,4]:

$$\Sigma_x = -\frac{\partial^2 V_\varphi}{\partial \eta_x^2}\ , \quad \Sigma_y = -\frac{\partial^2 V_\varphi}{\partial \eta_y^2}\ , \tag{11}$$

where: $\eta_x = k_x \rho_x$ and $\eta_y = k_y \rho_y$ are non-dimension parameters.

Knowledge of the phase correlation function allow to calculate broadening of temporal spectrum of a scattered radiation:

$$<\Omega^2> = -V_0^2 \left[V_\varphi''(\rho)\cos^2\theta_0 + \frac{V_\varphi'(\rho)}{\rho}\sin^2\theta_0 \right], \tag{12}$$

here: ρ is the distance between the observation points in the plane perpendicular to the direction of wave propagation, θ_0 is the angle between the vector $\tilde{\mathbf{n}}$ and the drift velocity $\mathbf{V_0}$ of the frozen in plasmonic structures. In this case new allocated direction is appeared – the velocity of the ionospheric irregularities. From equation (12) it is possible to calculate and measure horizontal drift velocity of the plasmonic structures if other parameters are known and vice-versa.

Phase fluctuations are responsible for fluctuations of the AOA which can be measured by interferometer systems. As a part of a radar propagation effects program at the Millstone Hill radar facility [10]. AOA has been measured with a single mono-pulse tracking system. Structure function $D_\varphi(\rho_x, \rho_y, L) = 2\left[V_\varphi(0,0,L) - V_\varphi(\rho_x, \rho_y, L)\right]$ allows to calculate AOAs in the main and perpendicular planes:

$$<\Theta_x^2> = \lim_{\eta_x \to 0} \frac{D_\varphi(\eta_x, 0, L)}{\eta_x^2},$$

$$<\Theta_y^2> = \lim_{\eta_y \to 0} \frac{D_\varphi(0, \eta_y, L)}{\eta_y^2}\ , \tag{13}$$

where: $\eta_x = k_0 \rho_x$ and $\eta_y = k_0 \rho_y$ are nondimensional parameters.

4. Numerical Calculations

Incident electromagnetic wave has frequency 3 MHz. Magnetoionic plasma parameters at the altitude of 260 km are: $u_0 = 0.22$, $\nu_0 = 0.28$, $\sigma_n^2 = 10^{-6}$ [11]. We will use the anisotropic power-law spectral correlation function of Ground-based radar system observations [12] showed that plasmonic structures in the terrestrial ionosphere having linear scales in the interval $(10\ \text{km} > \lambda > 100\ \text{m})$ are characterized by spectral indices in the range of -4.8 ± 0.2, both in the vertical horizontal directions. For irregularities in 20 m to 200 m scale size range spectral power could be presented by the Gaussian function. 3D spectral correlation of electron density irregularities combining anisotropic Gaussian and power-law spectra [13] is:

$$W_n(\mathbf{k}) = \frac{\sigma_n^2}{8\pi^{5/2}}\ \frac{A_p\, l_\parallel^3}{\chi^2\left[1 + l_\perp^2(k_x^2 + k_y^2) + l_\parallel^2\, k_z^2\right]^{p/2}} \cdot$$

$$\exp\left(-\frac{k_x^2\, l_\perp^2}{4} - p_1 \frac{k_y^2\, l_\parallel^2}{4} - p_2 \frac{k_z^2\, l_\parallel^2}{4} + p_3\, k_y\, k_z\, l_\parallel^2 \right), \tag{14}$$

where: σ_n^2 is the mean-square fractional deviation of electron density. This spectral function contains anisotropy factor $\chi = l_\parallel / l_\perp$ (the ratio of longitudinal and transverse linear sizes of ionospheric plasma irregularities), $p_1 = (\sin^2\gamma_0 + \chi^2\cos^2\gamma_0)^{-1}\left[1 + (\chi^2 - 1)^2 \cdot \sin^2\gamma_0 \cos^2\gamma_0\ \chi^{-2}\right]$, $p_2 = (\sin^2\gamma_0 + \chi^2\cos^2\gamma_0)/\chi^2$, $p_3 = (\chi^2 - 1)\sin\gamma_0\cos\gamma_0 (2\chi^2)^{-1}$, γ_0 is the orientation angle of elongated ionospheric plasma irregularities with respect to the magnetic lines of force; k_z indicates field aligned wave number. A spheroidal shape of plasmonic structures is caused due to the difference of the diffusion coefficients in the field aligned and field perpendicular directions. These irregularities are quite readily observable in the presence of strong artificial and/or natural perturbations in the terrestrial ionosphere.

Experimentally observable power-law spectral correlation function of the electron density fluctuations has the following form:

$$W_n(\mathbf{k}) = \frac{\sigma_n^2}{8\pi^{5/2}}\ \frac{A_p\, l_\parallel^3}{\chi^2\left[1 + l_\perp^2\,(k_x^2 + k_y^2) + l_\parallel^2\, k_z^2\right]^{p/2}}\ , \tag{15}$$

 DOI: https://doi.org/10.30564/jees.v2i1.1763

where: $A_p = \Gamma\left(\frac{p}{2}\right)\Gamma\left(\frac{5-p}{2}\right)\sin\left[\frac{(p-3)\pi}{2}\right]$, $\Gamma(x)$ is the gamma function. In the polar ionosphere geomagnetic field lines are oriented almost vertically formatting elongated vertical plasmonic structures. Characteristic spatial scale of electron density irregularities ranges from hundreds of meters to ten kilometers. The geomagnetic field of the high-latitude ionosphere plays an important role in the process of plasmonic structures generation. The incident electromagnetic wave propagating in the conductive randomly inhomogeneous ionospheric plasma makes angle θ with an external magnetic field in the main plane.

The solution of the biquadratic equation (5) at $s << \tilde{\sigma}_{ij}$ gives the attenuation of electromagnetic waves propagating in the homogeneous conductive collision magnetized plasma $\mathbf{E} \sim \exp(-i\,\mathbf{k}\,\mathbf{r}) = \exp(-i\,\mathbf{k}'\mathbf{r} + \mathbf{k}''\mathbf{r})$ We have four roots:

$$t_{1,2} = \pm\left[(1 - 0.02\sin^2\theta) + i\,0.16\cos^2\theta\right] \text{ and}$$

$$t_{3,4} = \pm\left[(0.3 - 1.64\sin^2\theta) - i\,0.9\,\sin^2\theta\right]. \quad (16)$$

Attenuation of electromagnetic waves in the conductive homogeneous plasma substantially depends on the refractive angle of the penetrated wave vector and the external magnetic field. For our model the imaginary part of t_i $(i = 1...4)$) varies from 0.41 up to 0.86 in the interval $0^0 \le \theta \le 90^0$.

One of the important problem of plasma turbulence in the upper ionosphere is the three–dimensional (3D) spatial spectra of the turbulence at various latitudinal regions describing the evolution of the statistical characteristics of scattered radiation. Spectral shape of irregularities in F–region of the ionosphere could be presented as a product of two functions having various dependencies on the wavenumber parallel $k_\parallel$ and perpendicular $\mathbf{k}_\perp$ to the geomagnetic field (the spectra have various inner scales in these directions). The spatial anisotropy of turbulence spectra for the geomagnetic north–south (N–S) and E–W directions has been studied in [14]. Cross-field anisotropy, whose scale is varying from $l_\perp > 0.5$ km to $l_\perp > 5 \div 10$ km plays a significant role in the phase fluctuations, where the N–S component of phase fluctuation spectra reaches the saturation. Irregularities of ionospheric F-region are strongly stretched along the geomagnetic field.

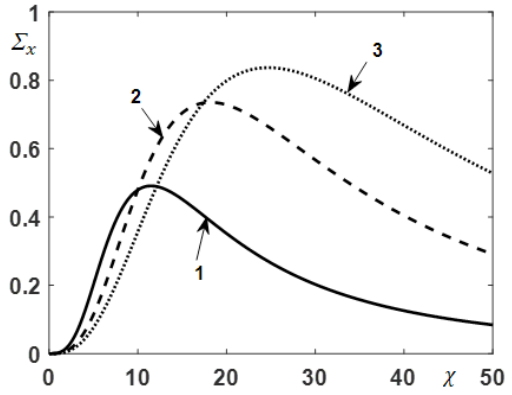

Figure 1. The broadening of the spatial power spectrum versus anisotoropy factor for different linear scales of ionospheric irregularities

Numerical calculation of the broadening of the SPS are carried out for the spectrum (14).

Figure 1 illustrates the broadening of the SPS of scattered electromagnetic waves for different characteristic spatial scales of elongated plasmonic structures: curve 1 corresponds to the $l_\parallel = 3$ km, curve 2 is devoted to the $l_\parallel = 6$ km, curve 3 - $l_\parallel = 9$ km at inclination angle of elongated ionospheric irregularities $\gamma_0 = 30^0$ and refraction angle of an incident wave $\theta = 30^0$. Increasing parameter $l_\parallel$, the SPS in the XOZ plane broadens and its maximum shifts to the right due to conductivity fluctuations. Maximum of the curve 1 is at $\chi = 11$, for curve 2 at $\chi = 18$, for curve 3 at $\chi = 25$.

Numerical analyses show that the broadening of the SPS decreases inversely proportion to the linear scale of ionospheric irregularities in the main YOZ plane due to both external magnetic field and longitudinal conductivity. Particularly, varying parameter in the interval $3 \le l_\parallel \le 9$ km, shift of maximum of the SPS is at $\chi = 4$, the broadening approximately is the same, but two order less than in the perpendicular XOZ plane.

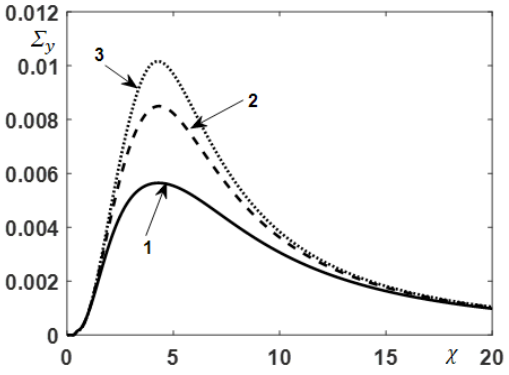

Figure 2. The broadening of the SPS versus anisotropy factor of elongated ireegularities for different inclination angle γ_0

DOI: https://doi.org/10.30564/jees.v2i1.1763

Figure 2 depicts the broadening of the SPS in the main YOZ plane. Curve 1 corresponds to the field-aligned $(\gamma_0 = 0^0)$ elongated ionospheric irregularities having characteristic linear scale $l_{\|} = 80$ km, refraction angle of an incident wave in the conductive collision turbulent magnetized plasma is equal to $\theta = 30^0$. Increasing angle in the interval $0^0 \le \gamma_0 \le 15^0$ broadening decreases, however maximum of these curves is at $\chi = 4$. That is for large-scale plasmonic structures inclination angle have no influence on the broadening of the SPS and shift of its maximum. Numerical calculations show that for the same parameters SPS substantially broadens: $\Sigma_x = 0.07$ at $\gamma_0 = 0^0$, while $\Sigma_x = 0.44$ at $\gamma_0 = 15^0$. All curves reach maximum at $\chi \approx 18$.

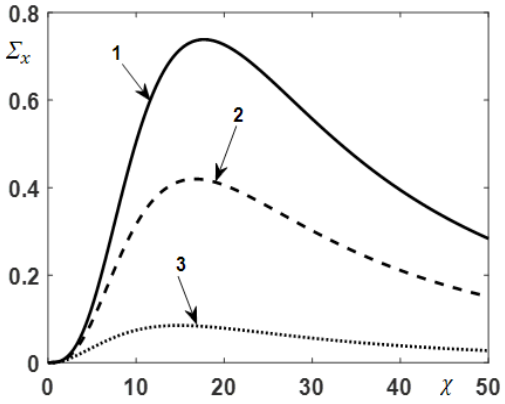

Figure 3. The broadening of the SPS versus anisotropy factor of elongated ireegularities for different refraction angle θ in the XOZ plane

Figure 3 illustrates the broadening of the SPS in the XOZ plane for plasmonic anisotropic structures having characteristic spatial scale 6 km, inclination angle $\gamma_0 = 15^0$ with respect to the geomagnetic lines of forces. Curve 1 is devoted to the refraction angle $\theta = 15^0$, curve 2 - $\theta = 30^0$, curve 3 - $\theta = 36^0$. Analyses show that the broadening of the SPS substantially depend on the refraction angle of penetrating incident electromagnetic wave in the conducive turbulent plasma: this statistical characteristic decreases $\Sigma_x = 0.74 \div 0.08$ inversely proportion to the angle $\theta = 15^0 \div 36^0$, maximums of these curves shift to the left $\chi = 18 \div 15$. In the YOZ plane for the same parameters ($\gamma_0 = 15^0$ and $l_{\|} = 6$ km) the broadening of the SPS less than in previous case: in the interval of the refraction angle $\theta = 8^0 \div 30^0$ the broadening in the main plane $\Sigma_y = 0.04 \div 0.01$, anisotropy factor is in the interval $\chi = 6 \div 4$.

The electron density irregularities were studied by measuring the intensity fluctuations at the frequencies 430 and 1400 MHz at the Arecibo Observatory [14]. It was found that large-scale electron density irregularities aligned with the geomagnetic field having dimensions longer than ~2 km along and several hundred meters across the geomagnetic field were formed in the F-region of the ionosphere. From the observed power spectra drift velocities of irregularities were observed. Since the irregularities are believed to be at a height of ~ 260 km the drift velocity of the irregularities ~ 46 m/sec (eastwards). Measurements of plasma drifts performed at Jicamarca show [15] that the zonal drift is westward and about 50 m/s during the day, and eastward and up to 130 m/s during the night.

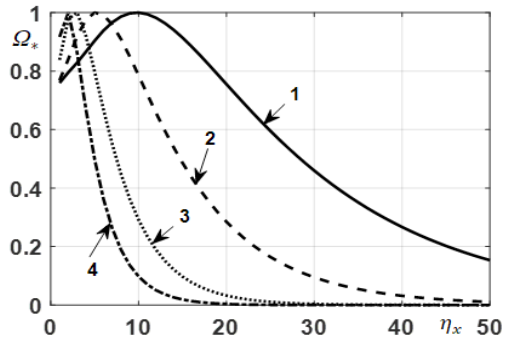

Figure 4. Broadening of the temporal spectrum versus distance between observation points for different anistoropy factor *x*

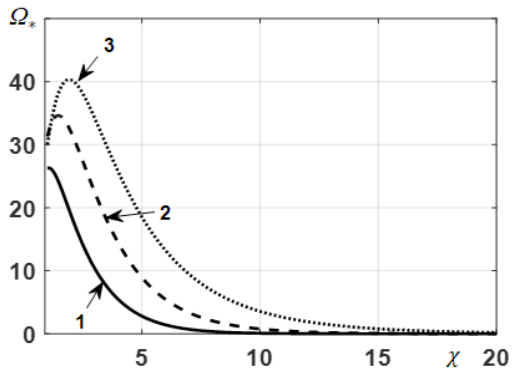

Figure 5. Broadening of the temporal spectrum versus anisotropy factor χ at different characteristic spatial scales of elongated plasmonic structures

Figure 4 illustrates the normalized temporal spectrum versus distance between observation points η_x in the XOZ plane for different anisotropy factors: $\chi = 5$ (curve 1), $\chi = 10$ (curve 2), $\chi = 20$ (curve 3), $\chi = 30$ (curve 4) for the power-law spectrum (15) at $\xi = 100$ (i.e. $l_{\|} = 16$ km). The width of the temporal spectrum narrows in proportion to the parameter χ in the perpendicular plane

Figure 5 depicts the broadening of the normalized temporal spectrum versus anisotropy factor at fixed distances between observation points $\eta_x = 30$, $\eta_y = 30$, $\theta = 30^0$ and different characteristic spatial scales of

 DOI: https://doi.org/10.30564/jees.v2i1.1763

ionospheric irregularities. Substituting equation (13) into (11) the normalized broadening of the temporal spectrum $\Omega_* \equiv <\Omega^2> / V_0^2$ is expressed via $K_{3/2}(x)$ McDonald function. Increasing drift velocity of the ionospheric elongated plasmonic structures, temporal spectrum of scattered electromagnetic waves broadens. Curve 1 corresponds to $\xi = 50$ ($l_{\|} = 800$ m), curve 2 is devoted to $\xi = 80$ ($l_{\|} = 1{,}3$ km), curve 3 - $\xi = 150$ ($l_{\|} = 2{,}4$ km). Increasing characteristic spatial scale of ionospheric irregularities from $l_{\|} = 800$ m up to $l_{\|} = 2{,}4$ km, temporal spectrum broadens 1.4 times

Temporal spectrum broadens in proportion to the refractive angle for large-scale plasmonic structures. Starting from $\chi = 1$ (isotropic case) temporal spectrum of scattered radiation increases, reaching maximums the curves smoothly decreases in proportion to the anisotropy factor of elongated ionospheric irregularities. The reason is that in the geometrical optics approximation, in non-absorbing medium (neglecting fluctuations) when both amplitude and phase Φ are real quantities, vector of the energy-flux density and the vector $\nabla\Phi$ are collinear and directed to the normal to the phase front, while in absorptive media (collision conductive magnetized plasma) the direction of wave propagation $\nabla\Phi_1$ and the direction of fast dumping of the wave $\nabla\Phi_2$ are not coincide [4]. On the other hand, according to the frozen-in hypothesis disregarding fluctuations of the drift velocity of ionospheric inhomogeneities, at transversal motion of inhomogeneities $V_\perp = 100$ m·s^{-1} the width of the spectrum $\Delta\Omega = V_\perp / \sqrt{\lambda L}$ is of the order of $\sim 3 \cdot 10^{-2}$ Hz which is in agreement with [16].

Phase structure function allow to calculate AOAs of scattered radiation in the conductive turbulent magnetized plasma for different orientation of the observation points. Numerical calculations are carrying out for experimentally observing power-law spectral function of electron density fluctuations using the experimental data. The AOA in the main and perpendicular planes are given by:

$$<\Theta_x^2> = \sigma_n^2 \frac{k_0 L \chi^2}{4\xi} \frac{D^2 + E^2}{1 + b^2 \chi^2},$$

$$\frac{<\Theta_y^2>}{<\Theta_x^2>} = \frac{\sqrt{\pi}}{8} \frac{1}{(1 + b^2 \chi^2)^2}. \qquad (15)$$

From this equation follows that the AOA in the XOZ plane exceeds the AOA in the main plane. Figure 5 and Figure 6 illustrate the dependence of the AOAs $\sqrt{<\Theta_{x,y}^2>}$ versus anisotropy factor χ at $\xi = 100$ ($l_{\|} = 1.6$ km). Curve 1 corresponds to the angle $\theta = 10^0$, curve 2 - $\theta = 12.5^0$, curve 3 - $\theta = 15^0$. Numerical calculations show that $\sqrt{<\Theta_x^2>}$ tends to the saturation starting at $\chi = 20$ (see Table 1), while $\sqrt{<\Theta_y^2>}$ has the asymmetric Gaussian form, reaching maximums the curves fast decrease. Particularly, at $\theta = 10^0$ the curve 1 reaches maximum at $\chi = 7.85$, $\sqrt{<\Theta_y^2>_{\max}} = 22'19''$; curve 2 has maximum at $\chi = 6.22$, $\sqrt{<\Theta_y^2>_{\max}} = 16'32''$; curve 3 has maximum at $\chi = 4.96$, $\sqrt{<\Theta_y^2>_{\max}} = 1'14''$. Increasing angle θ maximum of the AOA in the main plane decreases and shift to the left. External magnetic field has substantial influence on the AOA in the main plane. Table 1 illustrates AOA in both planes for plasmonic structures having characteristic spatial scale1.6 km, $k_0 L = 10^4$ (or L=160 km). Estimations show that conductivity fluctuations increase AOAs of scattered radiation in the polar terrestrial ionosphere.

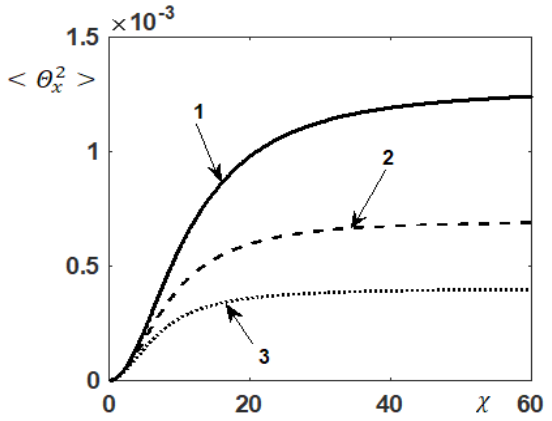

Figure 6. Angle-of-arrival in the XOZ plane versus anisotropy factor

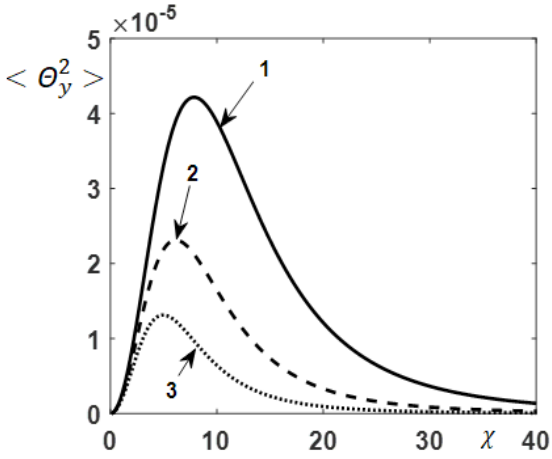

Figure 7. Angle-of arrival in the main plane versus parameter χ

DOI: https://doi.org/10.30564/jees.v2i1.1763

Table 1. Numerical calculations

χ	θ^0	$\sqrt{<\Theta_x^2>}$	$\sqrt{<\Theta_y^2>}$
10	10^0	$1^0\,22'$	$21'25''$
20	10^0	$1^0\,46'$	$11'58''$
30	10^0	$1^0\,53'$	$6'34''$
40	10^0	2^0	$4'13''$
χ	θ^0	$\sqrt{<\Theta_x^2>}$	$\sqrt{<\Theta_y^2>}$
10	15^0	$58'26''$	$8'42''$
20	15^0	$1^0\,8'$	$3'18''$
30	15^0	$1^0\,8'$	$1'37''$
40	15^0	$1^0\,8'$	$58''$

Numerical calculations of the AOAs were carried out for small-scale ionospheric irregularities having characteristic spatial scale $l_{\|} = 80$ m ($\xi = 5$) and $k_0 L = 2 \cdot 10^3$ (or L = 32 km). In this case at $\theta = 10^0$, $\chi = 8$, $\sqrt{<\Theta_y^2>_{\max}} = 44'41''$ at $\theta = 12^0$, $\chi = 6$, $\sqrt{<\Theta_y^2>_{\max}} = 35'4''$;at $\theta = 15^0$, $\chi = 5$, $\sqrt{<\Theta_y^2>_{\max}} = 24'45''$;at $\theta = 20^0$, $\chi = 3$, $\sqrt{<\Theta_y^2>_{\max}} = 14'6''$.

The behavior of the curves is the same than in the case of large-scale ionospheric irregularities. Study of the AOA could provide useful information about the structure of the ionospheric irregularities. Upper ionosphere places the important role in satellite communication over great distances.

5. Results and Discussion

The dispersion equation is obtained describing attenuation of oblique incident radio wave on a conductive collision homogeneous magnetized plasma in the polar terrestrial ionosphere. Second order statistical moments of scattered electromagnetic waves are calculated using the complex geometrical optics approximation.

Applying the phase structure function, the AOAs are calculated numerically for experimentally observing power-law spectral function of electron density fluctuations in the main and perpendicular planes using the experimental data. Numerical calculations of the AOA versus anisotropy factor were carry out for both small and large-scale ionospheric irregularities in the conductive polar ionospheric plasma. It was shown that the AOA in the main plane has the asymmetric Gaussian form; increasing refractive angle maximum of these curves shifts to the left, while the AOA in the perpendicular plane increases in proportion to the anisotropy factor and tends to the saturation. Estimations show that conductivity fluctuations increase AOAs of scattered radiation than in magnetized plasma with permittivity fluctuations. AOAs in the main plane are less than in perpendicular plane caused due to the existence of an external magnetic field and longitudinal conductivity. Study of the AOA could provide useful information about the structure of the ionospheric irregularities.

Frequency fluctuations of radio waves propagating in the conductive turbulent polar ionosphere is investigated. Correlation function of the phase fluctuations allows to calculate temporal spectrum of scattered radiation account being taken the drift velocity of elongated plasmonic structures. Temporal spectrum of scattered electromagnetic waves broadens Increasing velocity of a plasma stream. The broadening of the temporal spectrum depends on the characteristic spatial scale of ionospheric irregularities, anisotropy factor and the angle between the refractive wave and the external magnetic field. The width of the normalized temporal spectrum broadens in proportion to the linear scale of plasma irregularities (at fixed angle θ) and the angle θ (at fixed characteristic spatial scale of plasmonic structures). The obtained results allow to solve the reverse problem restoring distance of travelling frozen in irregularities in the polar conductive ionosphere for given drift velocity and the angle between the observation points and the direction of irregularities movement.

References

[1] Ishimaru, A. Wave Propagation and Scattering in Random Media, Vol. 2, Multiple Scattering, Turbulence, Rough Surfaces and Remote Sensing, IEEE Press, Piscataway, New Jersey, USA, 1997.

[2] Rytov, S.M., Kravtsov, Yu.A., Tatarskii, V.I., Principles of Statistical Radiophysics. vol.4. Waves Propagation Through Random Media. Berlin, New York, Springer, 1989.

[3] Jandieri, G.V., Ishimaru, A., Yasumoto, K., Khantadze, A.G., Jandieri, V.G. Angle-of Arrival of Radio Waves Scattered by Turbulent Collisional Magnetized Plasma Layer, International Journal of Microwave and Optical Technology, 2009, 4: 160-169.

[4] Jandieri, G.V., Gavrilenko, V.G., Sorokin, A.V., Jandieri, V.G. Some Peculiarities of the Angular Power Distribution of Electromagnetic Waves Multiply Scattered in a Collisional Magnetized Turbulent Plasma, Plasma Phyiscs Report. 2005, 31: 604-615.

[5] Aydoglu, M., Ozcan, O., Effect of magnetic dec-

 DOI: https://doi.org/10.30564/jees.v2i1.1763

lination on refractive index and wave polarization coefficients of electromagnetic waves in mid-latitude ionosphere, Indian Journal of Radio and Space Physics, 1996, 25: 163-270.

[6] Jandieri, G.V., Ishimaru, A., Rawat, Banmali, Mchedlishvili, N.I. Spatial power spectrum of scattered electromagnetic waves in the conductive anisotropic magnetized plasma, International Journal of Microwave and Optical Technology, 2019, 14: 440-449.

[7] Ginzburg, V.L. Propagation of Electromagnetic Waves in Plasma, Gordon and Beach, New York, 1961.

[8] Booker, H.G. Cold Plasma Waves, Martinus Nijhoff Publishers, Dordrecht-Boston-Lancaster, 1984.

[9] Jandieri, G.V., Ishimaru, A., Jandieri, V.G., Khantadze, A.G., Diasamidze, Zh.M. Model computations of angular power spectra for anisotropic absorptive turbulent magnetized plasma, Progress in Electromagnetics Research, 2007, 70: 307-328.

[10] Evans J.V. (Ed) Millstone Hill Radar Propagation Study: Calibration, Technical Report. 508, Linkoln Lab., Mass. Inst. Of Technol.-Lexington, 1973.

[11] Kravtsov, Yu.A. Feizulin, Z.I., A.G.. Vinogradov, Penetration of Radio Waves Through the Terrestrial Atmosphere, Radio and Communication, Moscow, 1983 (in Russian).

[12] Singh, M., Szuszczewicz, E.P. Composite equatorial spread F wave number spectra from medium to short wavelength, Journal of Geophysical Research, 1984, 89: 2313-2317.

[13] Jandieri, G., Ishimaru, A., Rawat, B., Kharshiladze, O, Diasamidze Zh.M. Power spectra of ionos-pheric scintillation, Advances Electromagnetics, 2017, 6:42-51.

[14] Frey, A., Gordon, W.E. HF produced ionospheric electron density irregularities diagnosed by UHF radio star scintillations, Journal of Atmosphere and Terrestrial Physics, 1982, 44: 1101-1111.

[15] Fejer B.G., Farley, D.T. Gonzales, C.A. Woodman, R.F., Calderon, C., F-region east-west drifts at Jicamarca, Journal of Geophysical Research, 1981, 86: 215-218.

[16] Kolosov, M.A., Armand, N.A., Yakovlev, O.I.. Propagation of Radio Waves at Cosmic communication, Moscow, Sviaz' 1969 (in Russian).

DOI: https://doi.org/10.30564/jees.v2i1.1763